



Together but separate: decoupled Variscan (late Carboniferous) and Alpine (Late Cretaceous - Paleogene) inversion tectonics in NW Poland

Piotr Krzywiec¹, Mateusz Kufraś¹, Paweł Poprawa², Stanisław Mazur³, Małgorzata Koperska⁴, Piotr Ślępek⁴

¹Institute of Geological Sciences, Polish Academy of Sciences, ul. Twarda 51/55, 00-818 Warsaw, Poland

²Faculty of Geology, Geophysics and Environmental Protection, AGH University of Science and Technology, al. Mickiewicza 30, 30-059 Kraków, Poland

³Institute of Geological Sciences, Polish Academy of Sciences, ul. Senacka 1, 31-002 Kraków, Poland

10 ⁴PGNiG S.A., Plac Staszica 9, 64-920 Piła, Poland

Correspondence to: Piotr Krzywiec (piotr.krzywiec@twarda.pan.pl)

Abstract. In Europe, formation of the Palaeozoic Variscan orogenic belt, and ~~then~~ the Mesozoic-Cenozoic Alpine-Carpathian orogenic belt led to a widespread inversion events within forelands of both orogenic domains. We used legacy 2D seismic data together with the newly acquired 3D seismic data that for the first time precisely imaged sub-Zechstein (i.e. sub-evaporitic) upper Palaeozoic succession in NW Poland in order to develop quantitative, balanced 2D model of the late Palaeozoic – recent evolution of this area, characterised by a complex pattern of repeated extension and inversion. Four main tectonic phases have been determined: (1) Late Devonian – early Carboniferous extension related to extensional reactivation of Caledonian thrusts, (2) late Carboniferous inversion caused by Variscan orogeny, (3) Permo-Mesozoic subsidence related to the development of the Polish Basin, and (4) ~~its~~ Late Cretaceous – Paleogene inversion. Variscan and Alpine structures form superimposed multilayer inversion system, mechanically decoupled along the Zechstein evaporites.

1 Introduction

Inversion tectonics has been intensely studied since the early 1980's, when a fully developed concept of sedimentary basin inversion, exemplified by a tectonic graben bounded by deeply rooted normal faults, was formulated (Glennie and Boegner, 1981; Bally, 1984). During this period, two dedicated volumes ~~have been~~ published in which geometry and evolution of inversion structures in different geodynamic settings were discussed (Cooper and Williams, 1989; Buchanan and Buchanan, 1995). Published case studies, documented by surface and subsurface data, were supplemented by numerous papers based on analogue and numerical modelling that focused on geometry of inversion systems, role of differential lithologies in formation of inversion structures, evolution of fracture systems ~~etc.~~ (e.g. Bonini et al., 2011; Buitter and Pfiffner, 2003; Buitter et al., 2006; Cloetingh et al., 2008; Dooley and Hudec, 2020; Henk & Nemčok, 2008; Jagger and McClay, 2018; McClay, 1995; Mitra and Islam 1994; Panien et al., 2005, 2006).



Thanks to all this work, the scene for inversion tectonics seems to be fairly well set; there are, however, still some problems that require further clarification. They also include crucial topics of inversion tectonics such as definition of inversion structures and their key characteristics. In fact, inversion structures come in various shapes and forms, and, despite all the studies briefly mentioned above, inversion tectonics could be quite differently understood. To some, it might be regarded as a general process that leads to reduction of the accommodation space and, eventually, cessation – or inversion - of the entire sedimentary basin. The process that reduces tectonic subsidence, eventually bringing it to halt and causing uplifts, might include reversal of basement normal faults that controlled localised tectonic subsidence as proposed in the classic model by Bally (1984). However, inversion tectonics could also involve other, sometimes very different processes such as salt movements, lithospheric buckling or isostatic adjustments (cf. Dewey, 1989; see also Kley, 2018; Krzywiec et al., 2018). Other, more “conservative” approach to inversion tectonics relies on the classic model by Bally (1984) that assumes (1) formation of tectonic half-graben bounded by normal fault(s) during extension, and (2) compressional reactivation of graben-bounding fault(s) and uplift of sedimentary infill deposited during extension (cf. also Cooper et al., 1989; Cooper and Warren, 2010, 2020; Tari et al., 2021; Williams et al., 1989). In this model, a master normal fault is deeply rooted in the crystalline basement so its reactivation under regional compression could be regarded as “thick-skinned inversion tectonics” (cf. Brun & Nalpas 1996). An extensional phase is documented by divergent pattern of the growth strata that are thickening towards the master fault. During inversion, formation of growth strata, characterized by local thinning, is focused above inversion anticlines that develop above the tip of inverted master fault (Fig. 1A). Well-documented examples of such deeply-rooted inversion structures include the Precambrian Calvert and Isa Basins from NE Australia (Gibson & Edwards 2020), the Devonian-Carboniferous Dnipro – Donetsk Basin (Maystrenko et al. 2003), the Triassic-Jurassic Lautaro Basin in N Chile (Martinez et al., 2012) or the Paleogene Song Hong and Beibuwan Basins in N Vietnam (Fyhn et al., 2018).

There are, however, numerous departures from this classic model of inversion tectonics. The most important difference might be the location of main basal detachment that can develop not within the crystalline basement, as proposed by Bally (1984), but within the pre-extensional sedimentary cover (Fig. 1B). A common situation in which such a location of the main detachment of an extensional–inversion system could be encountered is related to foreland thin-skinned fold-and-thrust belts, where major thrusts could be first reactivated as normal faults and then inverted due to regional compression (e.g. Di Domenico et al., 2014; Tavarnelli, 1999; Withjack et al., 2010). Thin- rather than thick-skinned character of inversion tectonics is in this case determined by a thin-skinned nature of the fold-and-thrust belt that undergoes reactivation (cf. Ivins et al., 1990). It is also worth noting here that extensional reactivation of thrusts is often referred to as a “negative inversion”, in contrast to “positive inversion” associated with reverse reactivation of normal faults that was briefly described above (e.g. Chadwick and Smith, 1988; Del Ventisette et al., 2021; Krantz, 1991; Tari et al., 2021; Tortorici et al., 2019). In this case however “inversion” seems to be used as an equivalent of “extensional reactivation” which is much broader term that does not fully comply with the original concept of “inversion tectonics” coined by Bally (1984). Bally’s original model was not



focused on inversion – i.e. reactivation – of basin-bounding faults but on inversion – i.e. partial or full destruction – of a sedimentary basin. Destruction of a sedimentary basin (half-graben) in Bally’s model is genetically linked to reactivation (reverse in this case) of a basin-bounding fault(s) but fault reactivation is a secondary process here while the main emphasis is on demise of half-graben formed during extensional phase (Bally, 1984). On the other hand, negative inversion might be
70 related to formation, not destruction, of a new basin that develops above extensionally reactivated thrust (e.g. Babaahmadi et al., 2018; Constenius, 1982, 1996; Powell and Williams, 1989; Tari et al., 2021; Velasco et al., 2010). Taking this into account it seems appropriate to delimit usage of the term “inversion tectonics” to “positive inversion” as originally proposed by Bally (1984), and to abandon the term “negative inversion” that in fact is related to rather different tectonic scenario.



75 The classic and relatively simple inversion scenario shown on Fig. 1 could be also greatly complicated by lithological variations of the sedimentary infill formed prior to onset of inversion i.e., prior, during and after extension. The most obvious example of influence exerted by lithology on inversion tectonics is the presence of ductile evaporites that leads to mechanical decoupling and formation of sub- and supra-salt / evaporitic structures, often of different geometries and kinematics (e.g., Brun and Nalpas, 1996; Dooley & Hudec 2020).

80

In Europe, formation of the Palaeozoic Variscan orogenic belt, and then the Mesozoic-Cenozoic Alpine-Carpathian orogenic belt led to a widespread inversion events within forelands of both orogenic domains. Variscan (i.e., late Carboniferous) inversion is well documented in areas where either suitable outcrops of deformed Palaeozoic rocks are present or deeper seismic imaging is not hampered by a thick Upper Permian (Zechstein) evaporitic cover, such as for example S UK or
85 France and Belgium. On the other hand, Alpine (i.e., Late Cretaceous – Paleogene) inversion is well documented by seismic reflection data that image usually complex supra-salt / supra-evaporitic thin-skinned structures that are however characterized by not always clear relationship to the sub-salt / sub-evaporitic deformations.

In this paper, we analyse complex inversion tectonics in NW Poland, where the superimposed effects of Variscan and Alpine
90 foreland compression led to formation of a multilayer decoupled inversion system. Our analysis is partly based on the newly acquired high-quality 3D seismic data that provided unique, so far unavailable insight into the pre-Zechstein sedimentary cover. Geometry, kinematics and casual links between consecutive phases of extension / subsidence and compression / inversion are discussed in a context of the regional Palaeozoic and Mesozoic evolution of Central and Eastern Europe.

2 Geological setting

95 The study area in NW Poland is located in the region, where crystalline basement is buried very deep, to a depth exceeding 11 km, as documented by deep seismic refraction data and gravity-magnetic modelling studies (Guterch et al., 1999; Guterch and Grad, 2006; Grad and Polkowski, 2016; Mazur et al., 2021). This is also compatible with the results of deep seismic



100 reflection surveying in the area adjacent to the east that documented the Caledonian orogenic front thrust over the undeformed lower Palaeozoic foreland and underlain by a lower plate that gradually descends towards the SW to a depth of at least 10 km (Krzywiec et al., 2014; cf. also Lazauskienė et al., 2002; Mazur et al., 2018; Poprawa, 2019, 2020; Poprawa et al., 1999). Structures analysed in this paper evolved above the frontal part of this deeply buried Caledonian thin-skinned orogenic belt (Mazur et al., 2016), below which the Precambrian suture of the Teisseyre – Tomquist Zone is located (Mazur et al., 2015).

105 The Caledonian orogenic belt in N Poland ceased to exist due to early Devonian uplift and widespread denudation (Dadlez, 1978; Poprawa, 2019). In the Variscan geological framework, the study area is located approximately 150 km NE from the front of the Variscan orogen that extends from south-western England across northern France, Belgium, northern Germany to Czech Republic, Poland and Western Ukraine, and then on to Romania, Bulgaria and Turkey (Fig. 2; e.g., Catalan et al., 2020; Franke, 2014; Kröner et al., 2008; Krzywiec and Kufraś, submitted; Laurent et al., 2021; Mazur et al., 2020; Okay and Topuz, 2017; Warr 2012). The most external part of the Variscan orogen i.e., the Rhenohercynian zone forms a foreland fold-and-thrust belt built of the deformed Devonian - Carboniferous sedimentary succession deposited along the southern margin of Laurussia and subjected to progressive thrusting and folding (Oncken et al. 1999). Final emplacement of the Variscan fold-and-thrust belt onto its foreland plate took place in the late Carboniferous (Kröner et al., 2008; Mazur et al., 2010, 2020). It led to the regional flexure of the foreland plate and formation of extensive Carboniferous foreland basin filled with a thick synorogenic sedimentary succession (Burgess and Gayer, 2000; Deckers and Rombaut, 2021; Franke, 2014; Kombrink et al., 2010; Leveridge and Hartley, 2006; Maynard et al., 1997; McCann, 1999; McCann et al., 2008; Narkiewicz, 2007, 2020; Opluštil and Cleal, 2007; Tomek et al., 2019). Final stages of evolution of the external Variscan fold-and-thrust belt were associated with a widespread inversion of Palaeozoic basins located within its foreland (e.g., Corfield et al., 1996; Glen et al., 2005; Peace & Besly, 1997; Pharaoh et al 2020; Shail & Leveridge 2009; Smith, 1999; von Hartmann, 2003). Until recently, no Variscan inversion structures have been recognized within the NE part of the Variscan foreland, including NW Poland, mainly because of low quality of sub-salt seismic imaging from the sub-Zechstein interval. Relatively intense compressional deformations were documented in the area devoid of the Zechstein evaporitic cover in SE Poland and western Ukraine within the Lublin – Lviv Basin (Krzywiec et al., 2017a,b; Kufraś et al., 2020; Tomaszczyk and Jaroński, 2017; Zayats, 2015) and adjacent areas including the Holy Cross Mountains (e.g., Czarnocki, 1957; Lamarche et al., 1999; Konon 2006, 2007). However, they have been recently interpreted as belonging to the frontal Variscan fold-and-thrust belt rather than being foreland inversion structures (Krzywiec et al., 2017a,b; Kufraś et al., 2020; Mazur et al., 2020).

130 The upper Palaeozoic sedimentary cover within the study area consists of the (upper Emsian–?) Middle Devonian to Mississippian sediments deposited within the Western Pomeranian Basin (Fig. 2, Fig. 3). This succession is composed of mainly clastic and carbonate sediments, with subordinate evaporites (Lipiec and Matyja, 1998; Narkiewicz, 2007, 2020;



Narkiewicz et al., 1998; Matyja, 1993, 1998, 2006, 2008; Muszyński et al., 1996). Late Devonian – early Carboniferous formation of sedimentary cover of Western Pomerania could be associated with regional extension and subsidence along the Laurussia southern margin (Smit et al., 2018).

135

The Pennsylvanian in the Western Pomeranian Basin is developed only locally in the northern part of the basin (Żelichowski, 1995; Matyja, 2006; Kuberska et al., 2007). ~~Also locally,~~ uppermost Carboniferous to lowermost Permian volcanic rocks have been encountered by wells (Maliszewska et al., 2016).

140 The Variscan foreland basin ceased to exist in the latest Carboniferous due to regional post-orogenic uplift and erosion (Edel et al., 2018; McCann et al., 2006; Ziegler, 1990). This was followed by renewed subsidence and sedimentation related to formation of an extensive Permo-Mesozoic basin that covered the large part of Europe (Doomenbal & Stevenson 2010, Littke et al 2008; Pharaoh et al., 2010; Scheck-Wenderoth et al., 2008; van Wees et al 2000; Ziegler, 1990). The Polish Basin together with its axial most subsiding part, the Mid-Polish Trough, formed the easternmost segment of this vast
145 sedimentary basin (Dadlez et al., 1995; Stephenson et al. 2003; Ziegler, 1990). The Polish Basin underwent long-term Mesozoic thermal subsidence, punctuated by three major pulses of extension-related accelerated tectonic subsidence: during late Permian to Early Triassic times, in the Late Jurassic (Oxfordian to Kimmeridgian), and in the early Cenomanian (Dadlez et al. 1995, Stephenson et al. 2003). Evolution of the NW and central segments of the Polish Basin, where a thick Zechstein evaporitic cover developed, was characterized by regional mechanical decoupling between the sub-Zechstein Rotliegend and
150 older substratum and the Mesozoic supra-Zechstein cover (cf. Krzywiec, 2006a,b; 2021; Krzywiec et al., 2006). This led to formation of a system of peripheral extensional structures located above the basin margins', including grabens or half-grabens detached in evaporites, and salt structures (Krzywiec, 2002a, 2012; Rowan and Krzywiec, 2014; Warsitzka et al., 2021).

155 Deposition in the Polish Basin started with the Rotliegend (Wordian – Wuchiapingian) continental clastic sediments that, however, are not present in the study area as it was located within the marginal part of the basin (Kiersnowski, 1998; Kiersnowski and Buniak, 2006; Krzywiec et al., 2017c). The Permian sedimentary cover of the area analysed in this paper is restricted to Zechstein (Wuchiapingian to Changshingian) evaporites (Wagner, 1994, 1998; Krzywiec et al., 2017c). They are overlain by a Triassic to Cretaceous clastic – carbonate sedimentary succession (cf. Dadlez and Marek, 1997; Krzywiec,
160 2006a; Ziegler, 1990).

The Polish Basin was inverted in the Late Cretaceous-Palaeogene (Dadlez et al., 1995, 1997; Głuszyński and Aleksandrowski, 2021; Krzywiec, 2002b, 2006b; Krzywiec et al., 2009; Resak et al. 2008). This was associated with widespread inversion of the European foreland triggered by the Alpine-Carpathian collision and Iberia-Europe convergence
165 (cf. Kley, 2018; Kley and Voigt, 2008; Kockel, 2003; Kossow and Krawczyk, 2002; Voigt et al., 2021; Mazur et al., 2005).



Inversion was associated with substantial uplift and erosion of the axial part of the Polish Basin i.e., the Mid-Polish Trough, which presently forms a regional anticlinal structure referred to as the Mid-Polish Anticlinorium (Swell), outlined by the Cenozoic subcrop of the Lower Cretaceous and older rocks (Fig. 4). Inversion commenced in the late Turonian and lasted until the Maastrichtian – Palaeocene (e.g. Krzywiec, 2002, 2006b; Krzywiec et al., 2018; Resak et al. 2008). Due to regional
170 inversion-driven uplift of the Mid-Polish Anticlinorium, the Upper Cretaceous mostly syn-inversion succession is presently preserved only along its both flanks. Increased Late Cretaceous subsidence, related to flexural bending of both flanks of the uplifted Mid-Polish Anticlinorium (cf. Hindle and Kley, 2020) and combined with globally high Cretaceous sea level, created relatively large accommodation space filled by syn-kinematic Upper Cretaceous strata. On the other hand, progressive growth of particular inversion structures, including also compressionally -reactivated salt diapirs, led to localised
175 reduction of accommodation space and erosion, associated with formation of growth strata characterised by thickness reductions, progressive unconformities and facies changes (Leszczyński, 2012, 2002; Krzywiec, 2002a, 2006b, 2012; Krzywiec and Stachowska, 2016; Krzywiec et al., 2009; 2018). Inversion-related uplift of the Mid-Polish Anticlinorium was associated with compressional reactivation of peripheral thin-skinned structures formed above the basin's flanks (e.g. Burliga et al., 2012; Krzywiec, 2002). The Koszalin - Chojnice Zone (Structure), located within the NE flank of the NW
180 segment of the Mid-Polish Anticlinorium (Fig. 5, Fig. 6) and analysed in this paper (see below), is one of such peripheral structures that underwent substantial inversion well documented by seismic data (cf. Krzywiec, 2006a,b).

The Cenozoic post-inversion unconsolidated, clastic sediments of small thickness, generally not exceeding 200 m, unconformably cover the Polish Basin (Piwocki and Kramarska, 2004; Jarosiński et al., 2009).

185 **3 Data and methods**

3.1 Seismic and well data

The seismic data used in this study included legacy 2D data and newly acquired 3D data. The regional seismo-geological transect shown on Figure 6 was assembled from several 2D profiles and, then, depth converted using velocity data from deep wells. The studied NE segment of this transects imaged the NE edge of the Mid-Polish Anticlinorium and the Koszalin -
190 Chojnice Structure – a peripheral structure developed within the NE flank of the Mid-Polish Trough / Anticlinorium. The 2D seismic data in this part of the basin, characterised by a relatively thin Zechstein cover, did image some structures within the sub-Zechstein succession, although low accuracy of seismic imaging and low resolution did not allow constructing a reliable geological model for the deeper substratum (Fig. 7A; cf. Antonowicz et al., 1994). A major breakthrough was related to acquisition of high-quality 3D seismic data that provided a clear sub-Zechstein image in the study area (Trela et al., 2011;
195 Fig. 7B). The seismic data was available in the depth domain and calibrated by several wells that, however, drilled the entire Permo-Mesozoic cover but encountered only the topmost part of the sub-Permian (i.e., sub-Zechstein) substratum, providing rather limited stratigraphic information on deeper seismic horizons within the Drzewiany Graben, excellently imaged by the



200

3.2 Structural restoration

Structural restoration was carried out along the cross-section that was located perpendicular to the strike of main structures imaged by the seismic data (Fig. 6). It was constructed using the NE part of the regional seismo-geological transect and two inlines extracted from the 3D survey that was located in the central part of the cross-section.

205

Standard kinematic algorithms such as fault-bend folding and simple shear were used in order to obtain a pre-deformational geometry of the horizons. Within the Drzewiany Graben, a shear angle was set to 50° and corresponds to the plane of maximum shear oriented parallel to minor normal fault surfaces (Dula, 1991; Xiao and Suppe, 1992). The relative timing of faults' activity was constrained based either on the presence of growth strata or cross-cutting relationships.

210

A maximum thickness of the syn-kinematic Upper Devonian – lower Carboniferous sedimentary sequence is deduced from the Drzewiany Graben, where it attains up to 4 km. Given that the most complete stratigraphic profile of the syn-kinematic strata is preserved within the SW part of the graben, it was used to approximate the currently missing portion of the Devonian–Carboniferous sedimentary rocks within the graben. Since little is known about a pre-deformation extent, geometry and thickness of the syn-tectonic strata at graben flanks, deposition of 50-m thick horizontal strata was assumed at each pre-inversion restoration step. It should be stressed though that, due to scarcity of data and widespread post-inversion erosion, reconstruction of the Devonian – Carboniferous cover outside the Drzewiany Graben was not the aim of this balancing exercise. The cross-sectional shape of the unconformity at the base Permian was approximated by a regional trend line that connects the local depressions along this horizon. Flattening of the reference line resulted in preserving morphology of the unconformity. The initial thickness of Cretaceous sedimentary sequence eroded after the Alpine inversion was reconstructed using published paleothickness maps (Leszczyński, 2002, 2012).

220

225

Modifications and improvements of the initial seismic interpretation were iteratively introduced until a satisfactory fit of the kinematic model to seismic and well data was achieved. The quality of the restored cross-section was verified via forward modelling by successive adding strain to the restored bed geometry, until the present-day shape of the horizons was obtained.



4 Results

4.1 Seismic and well data

Well D-2 calibrated the Permo-Mesozoic succession and provided partial stratigraphic information about the upper Palaeozoic infill of the Drzewiany Graben (Fig. 7C). It drilled Tournaisian strata within the hangingwall of the master fault of the graben, went through the fault, and encountered Frasnian – Famennian within the footwall. Upper Devonian was interpreted within the axial part of the graben using similarity of seismic horizons from the footwall and the hangingwall. Thickening of the large part of the sedimentary infill of the Drzewiany Graben towards the master fault suggests its syn-depositional activity during extension, similarly to the model shown on Figure 1. On the other hand, the present day geometry of the infill, in particular an anticline above the master fault, suggests substantial inversion (cf. Fig. 1).

2D data provided information on the regional present-day geometry of the Permo-Mesozoic succession along the NE edge of the Mid-Polish Anticlinorium (Fig. 6). The Koszalin - Chojnice Structure was interpreted as a thin-skinned anticlinal structure developed above the listric reverse fault rooted within the Zechstein evaporites, which is compatible with an overall geometry of this structure imaged by a large number of good-quality seismic data (cf. Krzywiec, 2006b, 2012; see also below).

4.2 Cross-section balancing

Cross-section restoration permitted to distinguish four major deformation events in the tectonic evolution of the Drzewiany Graben (Fig. 8). According to the most plausible scenario, the Drzewiany Graben formed in response to Late Devonian – early Carboniferous NE-SW-oriented horizontal extension (Fig. 8a-i). Tectonic activity of the two conjugate, oppositely-dipping graben-bounding normal faults created accommodation space successively filled with syn-tectonic deposits. A heterogeneous displacement along the master faults resulted in vertical variation in the geometry of growth strata within the graben: antithetic rotation and thickening toward the northeast is the most pronounced at the basal section of the syn-kinematic sedimentary sequence, as opposed to the youngest sub-parallel layers maintaining almost constant thicknesses (Fig. 8g-h). During the final stage of the extensional evolution of the Drzewiany Graben, the syn-tectonic strata were disrupted by secondary normal faults (Fig. 8i; cf. Jagger and McClay, 2018; McClay, 1995; McClay & Scott, 1991). The estimated total amount of the Late Devonian – early Carboniferous extension responsible for formation of the Drzewiany Graben was as high as 10 km (Fig. 8). However, this should be regarded as a minimum value as thickness of the post-Tournaisian strata that could have been deposited in this area is not known. In addition, the assumed thickness of the Tournaisian is a minimum estimate.



The following phase of the Variscan structural inversion affected ~~solely~~ the SW-dipping master fault by inducing 2 km of reverse displacement (Fig. 8j). The remaining normal faults do not show any seismic-scale signs of compressional reactivation. The syn-extensional sedimentary infill of the Drzewiany Graben, occupying a proximal portion of the hanging wall, was, then, folded due to material translation over the underlying concave master fault. As a result, an asymmetric, open anticline with c. 1.3 km of structural relief was produced (Fig. 8j). Its topmost part, together with growth strata that might have been deposited during inversion, was removed due to syn-to-post-inversion erosion.

The subsidence centre of the Polish Basin, illustrated on Figure 8l-o, developed SW from the analysed profile, within the Mid-Polish Trough, i.e., in the area, where currently the Mid-Polish Anticlinorium, formed by the second inversion event, is located (cf. Fig. 6). Subsidence within the Mid-Polish Trough led to tilt of the pre-Permian strata by c. 4° to the SW. It generated accommodation space that was successively filled in with sedimentary rocks thickening to the SW (i.e., towards the basin depocenter). Normal faulting related to the basin formation only slightly affected the study area by growth of new SW-dipping faults beneath the Zechstein evaporitic cover. It should be noted that faults outlining the inverted Drzewiany Graben were not reactivated during this tectonic phase. This deformation event yielded up to 500 m of horizontal stretching.

Evolution of the Permian-Mesozoic basin was terminated by the Late Cretaceous – Paleocene inversion that is the youngest major deformation stage discernible in the study area. It was caused by the NE-SW-oriented compression and formation of the thin-skinned anticlinal Koszalin – Chojnice Structure (Fig. 8q; cf. Krzywiec, 2006a, 2021). Its location might have been triggered by a buttressing effect of the sub-Zechstein basement steps related to small normal faults that were not reactivated during the inversion. Growth of the fault-related anticline was associated with c. 500 m of horizontal shortening. Post-inversion erosion removed the topmost part of the Koszalin – Chojnice Structure and part of the Upper Cretaceous syn-inversion cover. The Cenozoic post-inversion strata in this area are of negligible thickness and are not considered in this model.

280 **5 Discussion and conclusions**

The quantitative, balanced model that was prepared using seismic and well data from NW Poland depicted four main tectonic phases: (1) Late Devonian – early Carboniferous extension, (2) late Carboniferous inversion, (3) Permo-Mesozoic subsidence, and (4) Late Cretaceous – Paleogene inversion. Decoupling between two inversion events was caused by Zechstein evaporites. All these four phases will be discussed below in a regional context of geological evolution. Regional conceptual model depicting pre-Permian Palaeozoic evolution of the study area is shown on Figure 9. Its eastern part is based on regional seismic profile PI-5400 of the PolandSPAN[®] survey acquired above the Caledonian foredeep i.e. the Baltic Basin (Krzywiec et al., 2014; Mazur et al., 2016), its western part on seismic data presented in this paper.



Two questions could be posed regarding ~~phase (1) i.e.~~, the Late Devonian – early Carboniferous extension; why was it
290 focused in this area, and what was the ~~casual~~ regional mechanism that led to this event? As it was described above, the West
Pomerania Basin developed above the frontal part of the thin-skinned Caledonian orogenic belt (Krzywiec et al., 2014;
Mazur et al., 2016; see also Dadlez, 1978; Katzung et al., 1993; Podhalańska and Modliński, 2006; Znosko, 1965; Żaba and
Poprawa, 2006). Reactivation of thrust structures as normal faults has been well documented in various orogenic belts (e.g.,
Corti et al., 2006; Faccenna et al., 1995; Withjack et al., 2010). Often, such reactivation is associated with formation of half-
295 grabens with syn-kinematic deposition focused above hanging wall of such asymmetric extensional system, and formation of
growth strata characterised by divergent stratal pattern and thickening towards the master fault, as shown on middle panels
of Figure 1A and 1B (Babaahmadi et al., 2018; Constenius, 1982, 1996; Powell and Williams, 1989; Tari et al., 2021;
Velasco et al., 2010). As described by Ivins et al. (1990), dips of many normal faults shallowing with depth are caused by the
reactivation of pre-existing thrust faults of underlying thrust belts. All these features are compatible with characteristics of
300 extensional Late Devonian – early Carboniferous half-grabens illustrated on Fig. 8b-i, including both their syn-kinematic
sedimentary infill as well as geometry of the master fault that could have been inherited from the Caledonian thrust belt.
Extensional grabens of the same age have been widely documented in different parts of the extensionally reactivated
Caledonides (e.g. Braathen et al., 2002; Fossen, 2010; Koehl et al., 2018; Rowan and Jarvie, 2020; Séranne et al., 1989;
Stemmerik, 2000). Such grabens, very similar to the Drzewiany Graben, located above the Caledonian thin-skinned fold-
305 and-thrust belt, have been also documented using deep seismic data in the south-western Baltic Sea, NW from the Western
Pomerania Basin (Lassen et al., 2001). In NW Poland, extensional reactivation of low-angle thrusts of the Caledonian thin-
skinned orogenic wedge, characterised by rather large thickness, explains both a listric geometry of the master fault that
governed the evolution of the Drzewiany Graben as well as its thin-skinned character (Fig. 9; see also Fig. 1B). Late
Devonian – early Carboniferous extension that reactivated Caledonian orogenic wedge coincided with a regional extensional
310 phase that affected the southern margin of Laurussia (cf. Smit et al., 2016).

Inversion tectonics and reactivation of basement faults and fracture zones within the forelands of orogenic belts is a well-
known process (cf. Ziegler et al., 2002). Well documented examples include the Apennines (Costa et al., 2021; Scisciani,
2009), Andes (Delgado et al., 2012; Bilmes et al., 2013; Iaffa et al., 2011) and the Alps (Schori et al., 2021). Deformations
315 within the Variscan orogenic belt also have ~~their~~ expression within the Variscan foreland – a whole array of inverted faults
and basins in front of the Variscan belt have been documented in the S UK (Chadwick and Evans, 2005; Corfield et al.,
1996; Glen et al., 2005; Peace and Besly, 1997; Shail & Leveridge, 2009; Smith, 1999). Figure 10 shows an interpreted
seismic profile across the Eakring anticline that documents substantial Dinantian (Toumaïsan – Viséan) extension and
subsidence, followed by late Carboniferous Variscan inversion, post-inversion erosion, and Permo-Triassic sedimentation. In
320 this case, there was no Late Devonian extension although lack of deep wells and inferior seismic imaging at deeper level
probably does not preclude this. The Eakring anticline could be directly compared to the inverted Drzewiany Graben, both in



terms of an overall geometry and main stages of development of Variscan inversion structures. There are also similar sub-Zechstein Variscan structures imaged on seismic data in N Germany (von Hartmann, 2003).

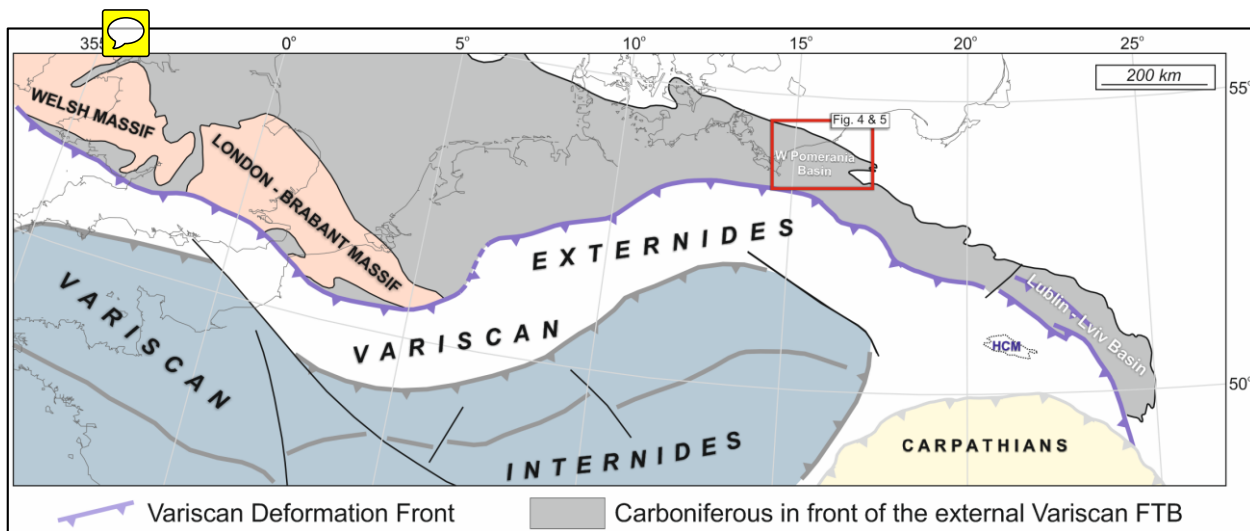
325 Late Cretaceous inversion in the vicinity of NW Poland has been documented by numerous authors (Deeks and Thomas, 1995; Krzywiec et al 2003; 2021; Mazur et al., 2005; Meissner et al., 2002; Sopher et al., 2016; Seidel et al., 2018; Deutschmann et al., 2018). Seismic examples from areas without Zechstein evaporites show deeply rooted reverse faults, along which basement blocks have been uplifted. However, different geometries are observed in the areas, where Zechstein evaporites were deposited. The evaporites led to regional mechanical decoupling between the sub-evaporitic basement and supra-evaporitic cover, both during extension as well as inversion (e.g. Ahlrichs et al., 2020; Betz et al., 1987; Burliga et al., 2012; Dooley and Hudec, 2020; Lohr et al., 2007; Marsh et al., 2010; Soto et al., 2007; Stewart, 1999; Withjack and Callaway, 2000). In our study area, a thin-skinned inversion structure – the Koszalin – Chojnice Structure – has been documented by seismic data. Due to deep post-inversion erosion, the top of this inversion anticline and associated inversion-related growth strata were removed. Better examples of the same structure are provided by seismic data from its more south-eastern segment, where relatively thick Upper Cretaceous succession is still preserved (Fig. 11A; cf. also Krzywiec, 2006b, 2012). Similar structures have been documented in S England (Chadwick and Evans, 2005). One of them is the Weymouth anticline, shown on Figure 11B. It evolved from Early Jurassic to Early Cretaceous due to detached thin-skinned listric normal faulting above the morphologically varied sub-salt basement. For this structure, Cenozoic (Miocene) inversion was postulated (Chadwick and Evans, 2005).

340 As it was described and illustrated above, the area analysed in this paper underwent two phases of inversion. Repeated extension and compression realized along the same faults have been described by many authors (e.g., Bosworth and Tari, 2021; Dichiarante et al., 2020; Minguely et al., 2010). In our case, the presence of Zechstein evaporites resulted in mechanical decoupling between the Devonian-Carboniferous and Triassic-Cretaceous levels, and, despite close location, both inversion structures evolved independently. Variscan inversion was associated with compressional reactivation of a listric normal fault that might have originally originated as a Caledonian thrust. Alpine (Late Cretaceous – Palaeocene) inversion was associated with listric thin-skinned reverse faulting detached within the Zechstein evaporites. Both inversion structures are compatible with certain elements of the classic inversion model by Bally (1984), but collectively form a complex, superimposed multilayer decoupled inversion system.

350

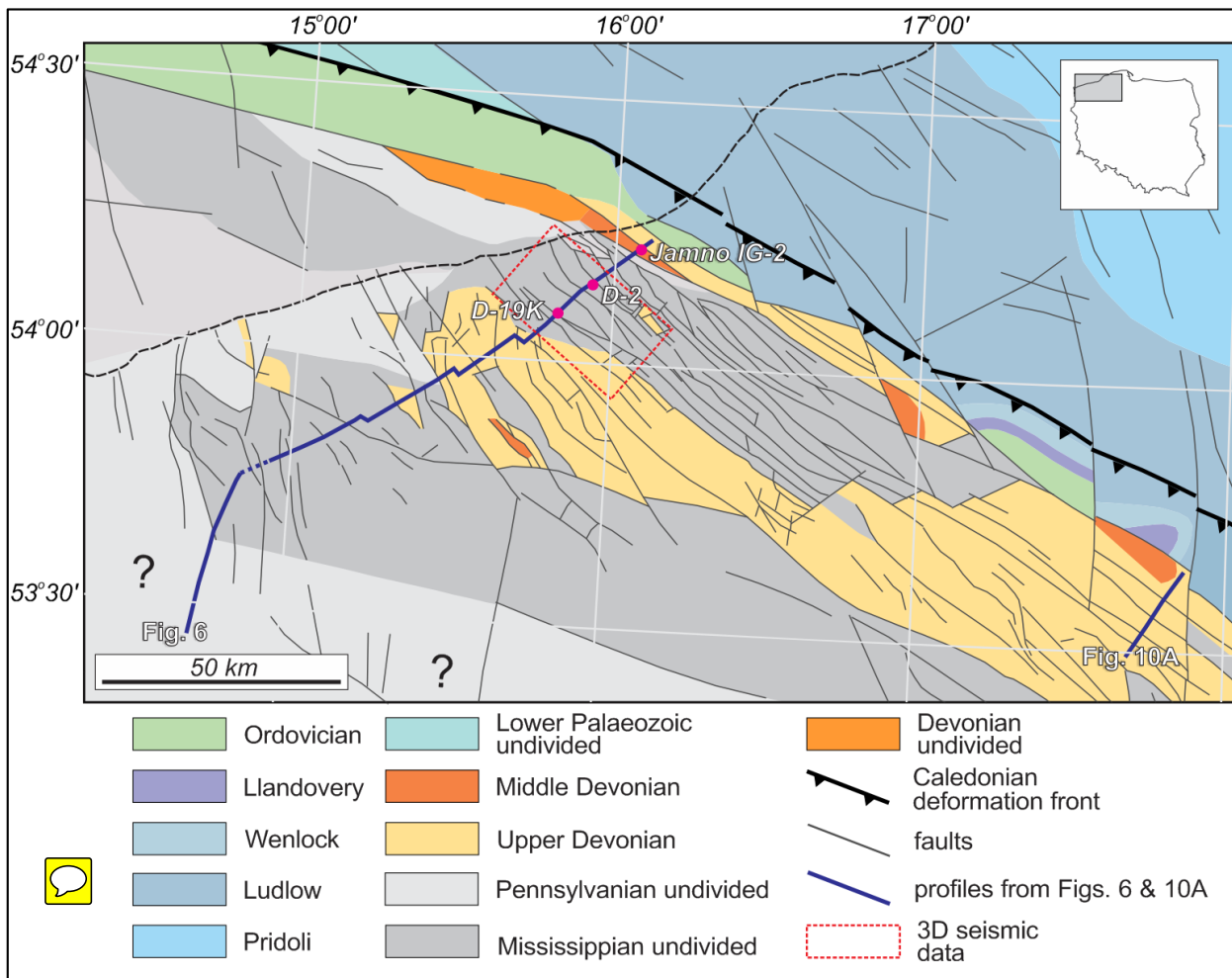


850



855

Figure 2: Regional map showing main elements of the Variscan orogenic belt and its foreland between the UK / France and Poland / Ukraine (adopted from Krzywiec and Kufraś, submitted, compiled after Mazur et al. 2020, Narkiewicz 2007, 2020, Opluštil and Cleal 2007; Ziegler 1990, Catalan et al. 2020). Grey area: present-day post-erosional extent of the Carboniferous basin. Variscan orogenic front (thick dark violet line) is shown as a foreland-verging thrust but it should be kept in mind that this is regional generalization meant to illustrate general vergence of the entire thrust belt and that along that front also backthrusting and wedging could be observed. HCM: Holy Cross Mountains.



860 **Figure 3:** Geological map of NW Poland without Permian, Mesozoic and Cenozoic (after Poprawa, 2019, supplemented).

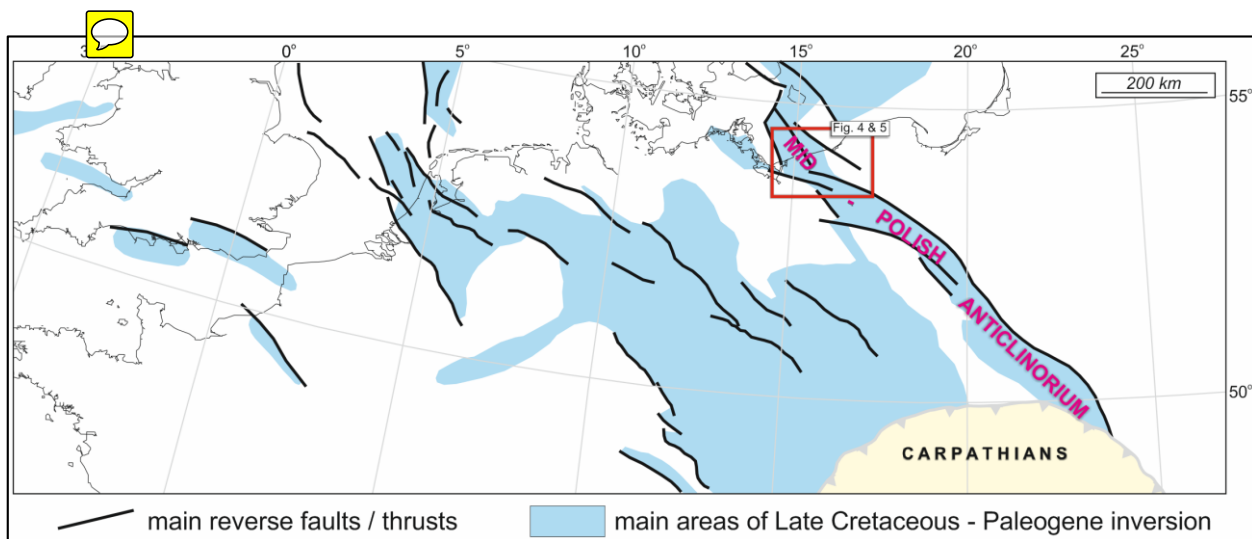


Figure 4: Schematic extent of the Alpine foreland inversion in Western and Central Europe, compiled after Kley (2018), Krzywiec et al., 2021; Voigt et al. (2021), Ziegler (1990) and Ziegler et al. (2002).